AIP Journal of Applied Physics

The conduction band absorption spectrum of interdiffused InGaAs/GaAs quantum dot infrared photodetectors

G. Jolley, I. McKerracher, L. Fu, H. H. Tan, and C. Jagadish

Citation: J. Appl. Phys. **111**, 123719 (2012); doi: 10.1063/1.4729833
View online: http://dx.doi.org/10.1063/1.4729833
View Table of Contents: http://jap.aip.org/resource/1/JAPIAU/v111/i12
Published by the American Institute of Physics.

Related Articles

Single photon emission in the red spectral range from a GaAs-based self-assembled quantum dot
Appl. Phys. Lett. 101, 103108 (2012)

Structural characterization of CdSe/ZnS quantum dots using medium energy ion scattering
Appl. Phys. Lett. 101, 023110 (2012)

Site-controlled formation of InAs/GaAs quantum-dot-in-nanowires for single photon emitters
Appl. Phys. Lett. 100, 263101 (2012)

Enhancement of the magneto-optical properties in 2-dimensional bilayered magnetic anti-dot lattice
Appl. Phys. Lett. 100, 222403 (2012)

Extremely high-density GaAs quantum dots grown by droplet epitaxy
Appl. Phys. Lett. 100, 212113 (2012)

Additional information on J. Appl. Phys.

Journal Homepage: http://jap.aip.org/
Journal Information: http://jap.aip.org/about/about_the_journal
Top downloads: http://jap.aip.org/features/most_downloaded
Information for Authors: http://jap.aip.org/authors

ADVERTISEMENT

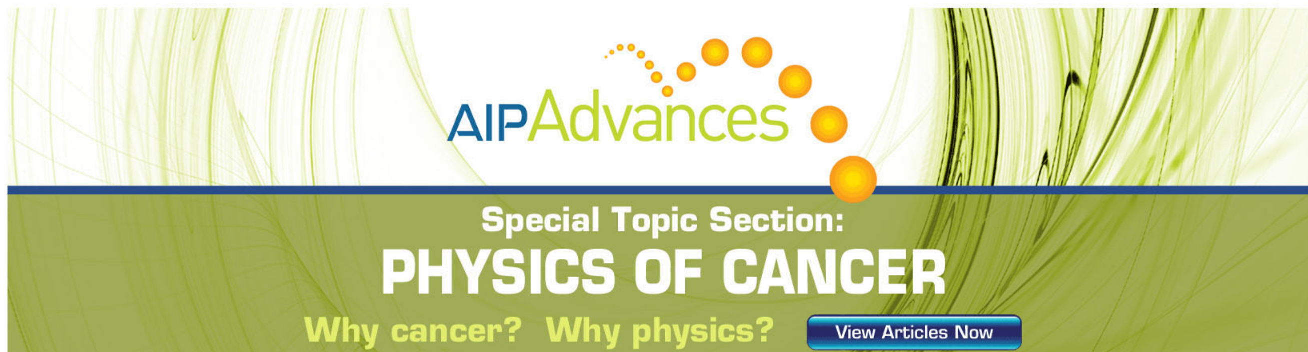

Downloaded 14 Sep 2012 to 150.203.178.114. Redistribution subject to AIP license or copyright; see http://jap.aip.org/about/rights_and_permissions

The conduction band absorption spectrum of interdiffused InGaAs/GaAs quantum dot infrared photodetectors

G. Jolley,[1,a)] I. McKerracher,[2] L. Fu,[2] H. H. Tan,[2] and C. Jagadish[2]
[1]*School of Electrical, Electronic and Computer Engineering, The University of Western Australia, Perth 6009, Australia*
[2]*Department of Electronic Materials Engineering, Research School of Physics and Engineering, The Australian National University, Canberra, ACT 0200, Australia*

(Received 20 February 2012; accepted 21 May 2012; published online 26 June 2012)

We report on a theoretical study of the relationship between interdiffusion and the conduction band optical absorption of In(Ga)As/GaAs quantum dots. Quantum dot geometries are progressively interdiffused based on Fick's model and the quantum dot strain, band structure and optical absorption cross-section are calculated numerically. Quantifying the effects of interdiffusion on quantum dot optical absorption is important for applications that utilize post-growth techniques such as selective area intermixing. © *2012 American Institute of Physics*.
[http://dx.doi.org/10.1063/1.4729833]

I. INTRODUCTION

The post-growth interdiffusion of self-assembled quantum dots (QDs) can be an important processing step in the fabrication of devices such as quantum dot infrared photodetectors (QDIPs) and QD lasers. Since it is difficult to control the size and shape of quantum dots through variations in the growth parameters, post-growth annealing can be an attractive method to optimize the band structure and tune the absorption spectrum.[1–7] Also, selective area interdiffusion can be utilized in the development of multi-colour infrared photodetectors and lasers.[8–10] Therefore, it seems worthwhile to quantify the relationship between interdiffusion and changes in the band structure and optical absorption of QDs. The theoretical dependence of quantum well band structure on interdiffusion has previously been evaluated in detail,[11–17] whereas there are far fewer studies on the effects of interdiffusion on QDs.[18–21] The three-dimensional carrier confinement and the large strain of self-assembled QDs result in a band structure and absorption spectrum that is considerably more complex.

Recently, Srujan *et al.*[18] investigated the effects of interdiffusion on the band structure of InAs/GaAs QDs to understand how annealing influences the photoluminescence spectrum. We build upon the work of Srujan *et al.* by evaluating the conduction band optical absorption and directly including the effect of QD strain on the band structure by solving a continuum elastic model with a finite element method. The general effects of interdiffusion on the energy levels and the absorption cross-section of various In(Ga)As/GaAs QD geometries are evaluated.

II. MODEL DETAILS

The interdiffusion of $In_xGa_{1-x}As$/GaAs QDs is modeled since this material system has been most widely used in the development of QD devices. In addition, the large QD strain can have an interesting dependence on interdiffusion which makes it worthwhile to study. It is straightforward to apply the single band effective mass model to the calculation of QD bandstructure and is known to have quite good accuracy for the conduction band states and is therefore chosen for this study. For a comparison of the single band model to the more accurate 8 band k.p model applied to InAs/GaAs QDs see Ref. 22. Since a single band effective mass calculation of the valence band is far less reliable, only calculations of the conduction band are performed. The conduction band edge potential is strongly affected by strain (predominantly the hydrostatic component of strain) which an accurate model of interdiffusion must take into consideration. Eigenstates of the following single band effective mass Hamiltonian including a correction due to strain are determined numerically by a basis function expansion method,

$$\hat{\mathrm{H}} = \left[-\frac{\hbar^2}{2}\nabla\cdot\frac{1}{m^*(\mathbf{r})}\nabla + V_{\mathrm{CBO}}(\mathbf{r}) + a_c(\mathbf{r})\varepsilon_{\mathrm{hyd}}(\mathbf{r})\right], \quad (1)$$

where $m^*(\mathbf{r})$ is the electron effective mass, $V_{\mathrm{CBO}}(\mathbf{r})$ is the conduction band-edge potential, $a_c(\mathbf{r})$ is the conduction band deformation parameter, and $\varepsilon_{\mathrm{hyd}}(\mathbf{r})$ is the hydrostatic component of strain. A given QD composition geometry is interdiffused based on Fick's model. After interdiffusion, a continuum elastic strain model is solved by a finite element method, from which $\varepsilon_{\mathrm{hyd}}(\mathbf{r})$ is obtained. Also, from the diffused material composition profile $m^*(\mathbf{r})$, $a_c(\mathbf{r})$, and $V_{\mathrm{CBO}}(\mathbf{r})$ are generated according to the equations,

$$m^*(\mathbf{r})/m_e = 0.067(1-x) + 0.04x, \quad (2)$$

$$V_{\mathrm{CBO}}(\mathbf{r}) = -0.89x - 0.477x(1.0-x) \quad (\mathrm{eV}), \quad (3)$$

$$a_c(\mathbf{r}) = -5.08x - 7.17(1.0-x) - 2.61x(1.0-x) \quad (\mathrm{eV}), \quad (4)$$

where m_e is the mass of an electron and x is the indium composition of $In_xGa_{1-x}As$. These are standard values[23] apart

a)Electronic mail: gregory.jolley@uwa.edu.au.

 © 2012 American Institute of Physics

Downloaded 14 Sep 2012 to 150.203.178.114. Redistribution subject to AIP license or copyright; see http://jap.aip.org/about/rights_and_permissions

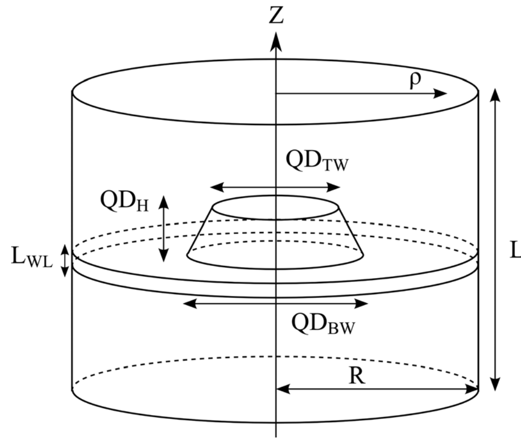

FIG. 1. The QD geometry and the dimensions of the calculation domain as used in the band structure calculations.

from the effective mass of InAs, for which a modified value of $0.04m_e$ is used to account for the effect of strain on the electron effective mass.[24] Quantum dots of a truncated cone shape (as depicted in Fig. 1) are studied which give the Hamiltonian a cylindrical symmetry allowing a reduction in the number of independent dimensions from 3 to 2. Since self-assembled In(Ga)As/GaAs QDs always form on a wetting layer (WL), it is also included in the model.

Wavefunctions are expanded as a sum of basis functions of the following form,

$$\chi^n_{j,m} = C_{n,j} J^n(k^n_j \rho/\mathrm{R}) \exp(i2\pi mz/\mathrm{L}) \exp(in\theta), \quad (5)$$

where $J^n(\rho)$ is the Bessel function of the first kind of integer order n, $J^n(k^n_j) = 0$ is the jth zero of the Bessel function and R is the calculation domain radius and L is its length. The integer n is the orbital angular momentum number, which due to the cylindrical symmetry is a good quantum number. This allows the calculation of QD eigenstates of any given angular momentum by setting the corresponding value of n. The $C_{n,j}$ terms are normalization constants,

$$C_{n,j} = \frac{1}{|J^{|n|+1}(k^n_j)|\mathrm{R}\sqrt{\pi \mathrm{L}}}. \quad (6)$$

The calculated energy eigenstates are labelled as, E^n_p, where p specifies the energy state number of those states with the orbital angular momentum number n. After the Hamiltonian matrix is diagonalized and the eigenstates are determined, the intersubband transition cross-section, σ, is calculated by applying Fermi's rule. The following equation is used to calculate the absorption cross-section,

$$\sigma(E) = \frac{2\pi e^2\hbar^2}{nc\varepsilon_0\omega}\left|\left\langle i\left|\frac{1}{2}\left(\frac{1}{m(\mathbf{r})^*}\varepsilon\cdot\nabla + \varepsilon\cdot\nabla\frac{1}{m(\mathbf{r})^*}\right)\right|f\right\rangle\right|^2 \quad (7)$$

$$\frac{1}{\Delta\sqrt{\pi}}\exp\left(-\frac{E_f - E_i - E}{\Delta}\right)^2, \quad (8)$$

where e is the charge of an electron, $n = 3.1$ is the refractive index of GaAs, c is the speed of light in vacuum, ε_0 is the free space permitivity, ω is the optical frequency of the transition, and ε is the polarization of light. To model the inhomogeneous line-width broadening due to a quantum dot size fluctuation, the Gaussian function $\frac{1}{\Delta\sqrt{\pi}}\exp(-((E_f - E_i - E)\ /\Delta)^2)$ replaces a delta function. For all calculations in this work, Δ is set to $21 \times (E_f - E_i)/E_{\mathrm{conf}}$ meV for all transitions that are bound-to-bound (BB), where E_{conf} is the energy of the QD ground state with respect to the unstrained GaAs conduction band-edge. For all bound-to-continuum (BC) transitions, Δ is set to 21 meV, giving a FWHM of 35 meV. Often a modified version of Eq. (7) is used to calculate the absorption spectrum of QWs and QDs in which $m^*(\mathbf{r})$ is set to a constant value equal to the QW or QD material, $m^*(\mathbf{r}) = m^*_{\mathrm{QW/QD}}$.[25] The justification being that only the effective mass of this region is important since the ground state wave function is mostly confined to this region. For interdiffused QDs, the effective mass becomes position dependent throughout the QD region and therefore it is not clear as to what value to adopt for m^*_{QD}. Equation (7) overcomes this difficulty and is symmetric under the interchange of the initial and final states which is expected to be a physical requirement.

Since the QD base width is significantly larger than the height, the absorption spectrum for light that is polarized in the z-direction is substantially different for light that is polarized in the radial plane and calculations have been performed for both polarizations. The size of the calculation domain (L and R) can influence the optical absorption spectrum, particularly for transitions to the GaAs barrier states. For all QD geometries, calculations have been performed to ensure that L and R are sufficiently large to have minimal influence on the absorption spectrum.

III. RESULTS AND DISCUSSION

Depending on the growth technique and parameters, self-assembled In(Ga)As/GaAs QDs of a limited range of sizes and shapes can be grown. Usually, the QD base width ($\mathrm{QD_{BW}}$) is within the range of 15-25 nm and the height ($\mathrm{QD_H}$) is between 3 and 7 nm.[26,27] Throughout this work, calculations are performed for 3 different QD geometries (QD1-QD3) as listed in Table I. The geometries of QD1 and QD3 have been chosen to result in a larger confinement energy which results in z-polarized optical transitions from the QD ground state to excited states that are bound. QD2 has a smaller confinement energy leading to dominant optical transitions to excited states that are non-bound GaAs barrier states. QD1 and QD2 are $\mathrm{In_{0.5}Ga_{0.5}As/GaAs}$ QDs whereas QD3 is comprised of InAs.

Before studying the effects of interdiffusion, an understanding of the band structures of QD1 is first sought. The absorption cross section and the potential profile as modified by strain of QD1 are shown in Figure 2. Strain significantly

TABLE I. The geometries of the 3 QDs that are studied in this work.

	$\mathrm{QD_{BW}}$ (nm)	$\mathrm{QD_{TW}}$ (nm)	$\mathrm{QD_H}$ (nm)	$\mathrm{L_{WL}}$ (nm)	In frac
QD1	18	10	7	1	0.5
QD2	18	10	5	1	0.5
QD3	15	7	8	0.5	1.0

Downloaded 14 Sep 2012 to 150.203.178.114. Redistribution subject to AIP license or copyright; see http://jap.aip.org/about/rights_and_permissions

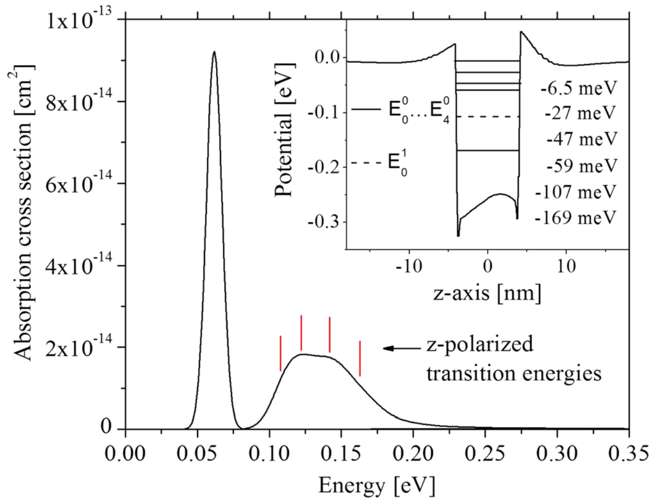

FIG. 2. The intersubband optical absorption cross section of QD1 for both radial and z-polarized light. The location of the first four z-polarized transition energies is indicated. Shown in the inset is the effective potential through the center of the QD and the location of the energy states that strongly feature in the optical absorption.

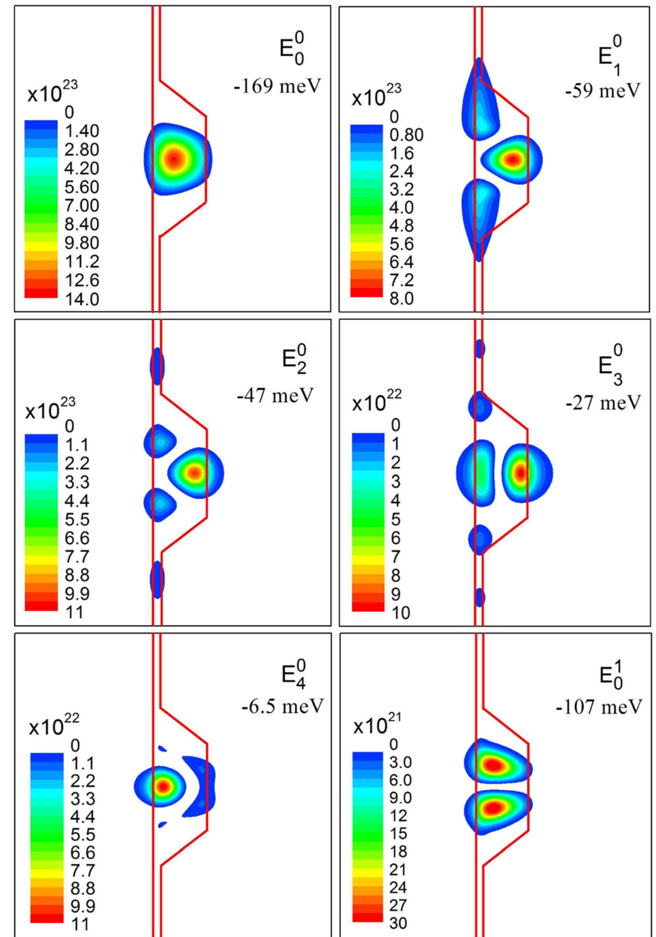

FIG. 3. The square of the wavefunction magnitude of the QD1 eigenstates that predominantly feature in the optical absorption cross section.

increases the QD potential and reduces the offset of the GaAs barrier and QD region from a value of -0.56 eV to an average value of about -0.27 eV. The effect of strain makes it difficult to grow In(Ga)As/GaAs QDs with a deep confinement energy. The first four excited energy states $E_1^0, \cdots E_4^0$ contribute significantly to the z-polarized absorption spectrum. Only the E_0^1 state contributes to the normal incidence absorption spectrum. Plots of these wavefunctions are shown in Fig. 3. In the case of QD1, the lack of symmetry in the z-direction and the presence of the WL result in z-polarized optical absorption to wavefunctions that display simultaneous oscillations in the radial and z-directions. Absorption occurs to states with wavefunctions that occupy both the WL and the QD. If the size of the calculation domain was infinite these states would form a continuous band. The higher energy states E_3^0 and E_4^0 are similar to E_1^0 and E_2^0 in that a large proportion of the wavefunction occupies the WL and displays oscillations in the radial direction, however, they also have a more prominent oscillation in the z-direction within the QD region. The net effect of the WL and the lack of symmetry in z-direction are a broad absorption peak with a FWHM of 63 meV. This is much larger than the FWHM of 35 meV which is imposed upon bound-to-continuum transitions by the computational routines. The Thomas-Reiche-Kuhn f-sum rule which is typically applied to atomic optical transitions states that the total integrated absorption strength for an atomic transition is equal to a constant value,

$$\sum_f \frac{2m_e\omega_{fi}}{\hbar}|\langle f|\hat{x}|i\rangle|^2 = 1, \tag{9}$$

where the summation is over all possible final states, $|f\rangle$ and $\omega_{fi} = (E_f - E_i)/\hbar$ is the transition frequency. Within the single band effective mass model, the f-sum rule also applies to semiconductor intersubband optical transitions. For a semiconductor structure with a constant effective mass, the absorption cross-section when integrated with respect to energy is equal to $(\pi e^2\hbar)/(nc\varepsilon_0 m^*)$. For a QD where the ground state wavefunction mostly occupies the QD region, the integrated absorption cross section will be close to this value, for which $m^* = m^*_{\mathrm{QD}}$. Therefore, the QD geometry has minimal impact upon the total absorption strength. However, if part of the absorption spectrum correlates to final energy states that are strongly bound to the QD/WL, then carrier escape can be inhibited. This can result in a reduction of the internal quantum efficiency of a QDIP. The normal incidence absorption spectrum is completely dominated by transitions to the lowest energy $n=1$ state (E_0^1). The very good spatial overlap between the E_0^0 and the E_0^1 states determines that the E_0^1 state is the only one that has a significant oscillator strength with E_0^0 for x-y polarized light. The E_0^1 state is strongly bound to the QD and therefore QDIPs do not usually register a photocurrent from this state. The f-sum rule implies that for the typical QD densities obtained by self-assembled growth (few 10^{10} cm^{-2}), the large responsivities (>1 A/W) reported for some QDIPs[28–33] is most certainly due to a larger photoelectric gain. For example, 10 QD layers with a sheet density of 5×10^{10} cm^{-2} per layer will have a peak absorption of at most approximately 0.76% for an absorption linewidth of 35 meV and a QD effective mass of 0.04 m_e. A potential enhancement to a QDIP photoresponse occurs by light taking multiple passes through the active

Downloaded 14 Sep 2012 to 150.203.178.114. Redistribution subject to AIP license or copyright; see http://jap.aip.org/about/rights_and_permissions

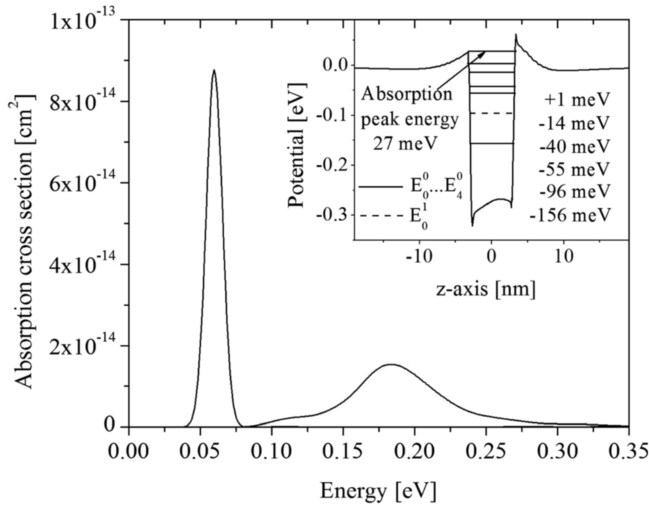

FIG. 4. The intersubband optical absorption cross section of QD2 for both radial and z-polarized light. Shown in the inset is the effective potential through the center of the QD and the location of some energy states.

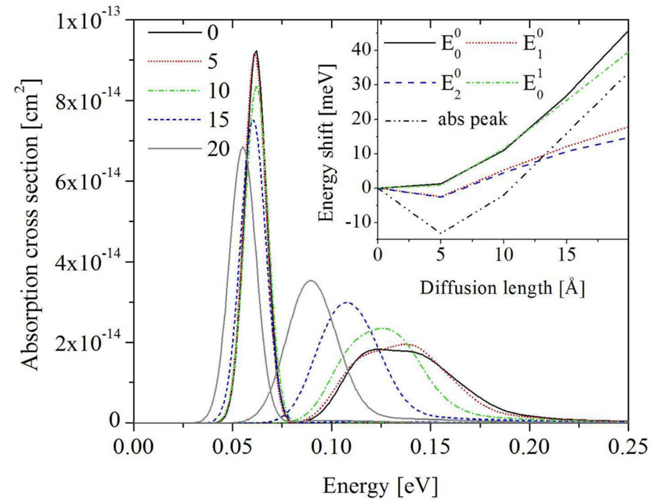

FIG. 5. The radial and z-polarized absorption cross section of QD1 for various diffusion lengths. The inset displays the energy shifts of the lower energy states and absorption peak energy as a function of diffusion length.

region. Incident light which is not absorbed on the first pass can reach the back of a semi-insulating substrate and reflect back towards the active region, possibly resulting in numerous passes by total internal reflection.[33]

The band structure of QD2 has similar features to QD1, the main difference being that z-polarized light predominantly induces transitions between the QD ground state and a band of GaAs barrier states. The absorption spectrum and conduction band diagram are shown in Figure 4. The absorption peak occurs at an energy that is 27 meV above the unstrained GaAs barrier potential, which is quite a large value and is partly due to the modification that strain makes to the GaAs barrier potential in the vicinity of the QD as evident in the inset of Fig. 4. This sort of effect can result in excessive dark current for a QDIP device since the barrier to the thermionic emission of electrons can be significantly less than the absorption peak energy, particularly if dark current electrons are emitted from the WL or tunnel through the thin region of GaAs barrier material surrounding the QD that has an increased potential due to strain. The FWHM of the z-polarized absorption peak of QD2 is very similar to QD1 with a value of 63 meV. It is interesting to note that the energies of the QD1 $E_0^0 \cdots E_4^0$ states are very similar to those of QD2 compared to the much large absorption peak energy of QD2 for z-polarized light. Transitions to a band of states with wavefunctions that occupy the WL which occur for QD1, also occur for QD2, however, the total absorption cross section to these states is much weaker since the z-dipole of these states is reduced due to the smaller height of QD2. This causes the absorption peak of QD2 to occur at a larger energy. The calculated absorption spectra of the single band model generally correlate well with measured values of QDIPs with similar QD geometries. For example, the peak energy of QD2 of 0.184 eV (6.76 μm) is very similar to the measured absorption peak energy of the 0.211 eV (5.9 μm) of the $In_{0.5}Ga_{0.5}As/GaAs$ QDIP reported in Ref. 34.

A. Interdiffusion

The QD interdiffusion is assumed to obey Fick's law which is given by,

$$\frac{\partial C(\mathbf{r},t)}{\partial t} = D\nabla^2 C(\mathbf{r},t), \tag{10}$$

where C is the concentration of some material type (in this case indium) and D is the diffusion constant. The amount of interdiffusion can be specified by a diffusion length, dl,

$$dl = \sqrt{TD}, \tag{11}$$

where T is the time over which the material is diffused. The optical absorption cross sections of QD1 and QD2 for various diffusion lengths are shown in Figs. 5 and 6, respectively. The differential energy shifts of the lower energy

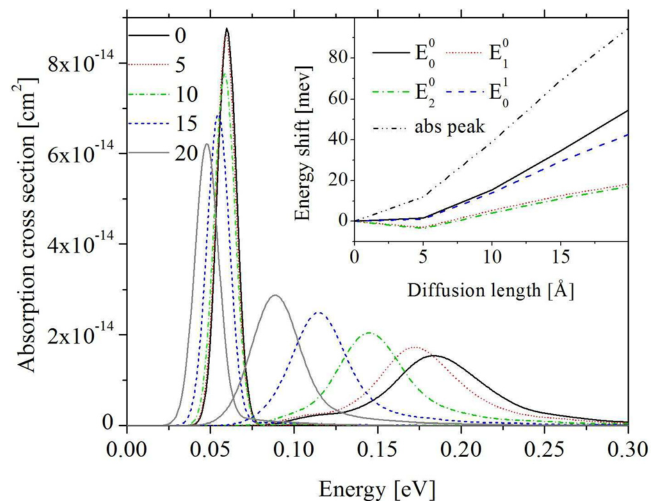

FIG. 6. The radial and z-polarized absorption cross section of QD2 diffused by various diffusion lengths. The inset displays the energy shifts of some energy states and the absorption peak energy as a function of diffusion length.

Downloaded 14 Sep 2012 to 150.203.178.114. Redistribution subject to AIP license or copyright; see http://jap.aip.org/about/rights_and_permissions

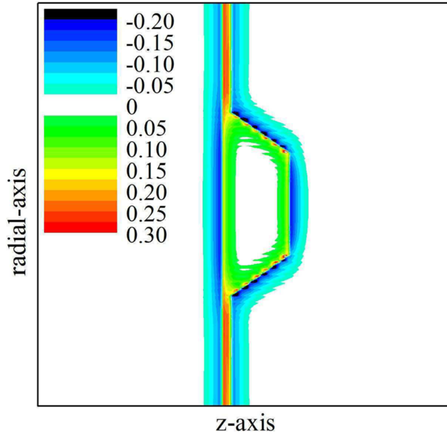

FIG. 7. The modification of the potential of QD1 due to diffusion length of 10 Å. The potential profile is taken through the center of the QD.

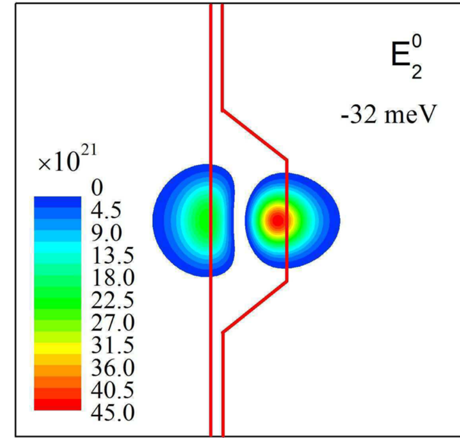

FIG. 8. QD1 wavefunction of the E_2^0 state for a diffusion length of 20 Å.

states as a function of interdiffusion are also shown in the inset figures. Clearly, interdiffusion can induce large energy shifts in the spectral response, particularly for z-polarized light.

Interdiffusion alters the QD effective mass Hamiltonian through three main mechanisms. The change in QD composition induced by interdiffusion directly alters the effective mass and unstrained potential. Interdiffusion also alters strain and therefore the influence that strain has on the conduction band potential. The effect of a small amount of interdiffusion on QD energy levels can be understood through time-independent first-order perturbation theory,

$$\Delta E = \langle \psi | \hat{\mathrm{H}}' - \hat{\mathrm{H}} | \psi \rangle, \quad (12)$$

where ψ is the envelope wavefunction of a state of interest, ΔE is the 1st order change in energy, and $\hat{\mathrm{H}}'$ is the Hamiltonian of the interdiffused QD.

$$\Delta E = \left\langle \psi \middle| V'(\mathbf{r}) - V(\mathbf{r}) + \frac{\hbar^2}{2} \nabla \frac{m(\mathbf{r})^* - m'(\mathbf{r})^*}{m(\mathbf{r})^* m'(\mathbf{r})^*} \nabla \middle| \psi \right\rangle, \quad (13)$$

where $V'(\mathbf{r})$ and $m'(\mathbf{r})^*$ are the strained conduction band potential and effective mass of the interdiffused QD, respectively.

Figure 7 displays $\Delta V = V' - V$ of QD1 with a diffusion length of 10 Å. It can be seen that the $\Delta V(\mathbf{r})$ function is positive within the QD region and negative within the surrounding region. Since the sign of ΔV changes across the QD boundary, the first order change in energy of an eigenstate depends on the rate of change of the magnitude of the wavefunction within the vicinity of the QD/barrier interface, where the interdiffusion occurs. The QD ground state wavefunction decays most rapidly into the GaAs barrier and therefore its energy is sensitive to interdiffusion. Although the excited states have wavefunctions with a greater magnitude at the QD/barrier interface, they have a reduced sensitivity because the rate of wavefunction decay into the barrier is less. Also, changes in the conduction band potential induced by interdiffusion are greater for regions outside of the QD boundary, compared with regions within the QD boundary. This is partially due to the nonlinear dependence of the unstrained $In_xGa_{1-x}As$ conduction band potential on the indium fraction. Therefore, the decrease in potential for regions outside of the QD exceeds the increase for regions within the QD boundary which leads to a reduced sensitivity of the excited state energies on interdiffusion. In addition, interdiffusion increases the effective mass for regions within the QD which has a tendency to decrease the energy of bound states. In addition to energy level shifts, interdiffusion influences the absorption spectrum by changing the oscillator strength of the individual transitions. For example, a diffusion length of 20 Å causes a reduction of QD1's z-polarized spectral response FWHM from 63 meV to 29 meV and a single excited state (E_2^0) is found to dominate the absorption cross section. Since the WL is thin, interdiffusion causes a very fast increase of its potential. Therefore, the band of states with wavefunctions that occupy the WL increase in energy and have a smaller energy range. In effect, the symmetry of the QD in the z-direction increases. The net result is that a single state with a large z-dipole dominates the absorption spectrum. A plot of the E_2^0 state which dominates the absorption spectrum of QD1 for a diffusion length of 20 Å is shown in Figure 8. The nature of this wavefunction can be compared with the E_2^0 state for an undiffused QD1 (Figure 3).

It is interesting to note that with a large diffusion length of 20 Å, the nature of QD2 transitions induced by z-polarized light change from bound-to-continuum to bound-to-bound. Similar to QD1, for a diffusion length of 20 Å, a single quasi-bound state (E_3^0) dominates the absorption spectrum of QD2. This leads to a reduction of the spectral response FWHM from 63 meV to 34 meV. In addition, the reduction of the absorption peak energy far exceeds the change in energy of the QD ground state since the final state energy for large diffusion lengths is 12 meV below the unstrained GaAs barrier band edge, whereas the absorption peak of non-interdiffused QD2 is 27 meV above the unstrained barrier band edge. For large diffusion lengths, the QD potential becomes spread out in the z-direction and therefore a bound excited state with a large z-dipole is supported. The larger strain of InAs/GaAs QDs has a stronger effect on the energy level dependence on

Downloaded 14 Sep 2012 to 150.203.178.114. Redistribution subject to AIP license or copyright; see http://jap.aip.org/about/rights_and_permissions

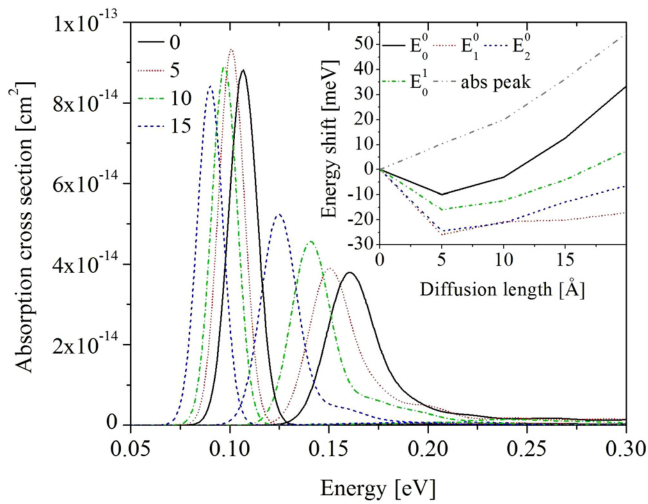

FIG. 9. The z and radially polarized optical absorption spectral of QD3 for various diffusion lengths. The inset figure displays the differential shifts in the lowest 4 energy levels and the absorption peak energy.

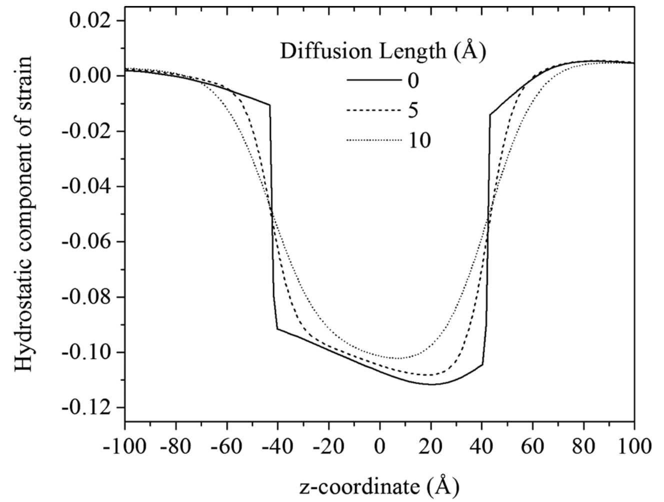

FIG. 11. The hydrostatic component of strain of QD3 for various diffusion lengths. Interdiffusion induces a relaxation of strain in excess of the changes in the composition for regions in the center of the QD.

interdiffusion. Shown in Figure 9 is the absorption spectrum of QD3 for various diffusion lengths and the differential change in the energy of a few states. Small amounts of interdiffusion actually result in a reduction in the QD ground state energy and excited states show a reduction in energy over a larger range of interdiffusion. A decrease in energy with interdiffusion is unexpected and is partially attributed to QD strain relaxation. Figure 10 is a plot of the change in potential of QD3 due to a diffusion length of 10 Å. The change in potential within the center of the QD is negative which has a tendency to reduce the energy of states that occupy this region. The results of strain calculations as shown in Figure 11 indicate that interdiffusion reduces the hydrostatic strain within the center of the QD even for regions of the QD that have no significant amounts of intermixing. For all three QDs, the normal incidence spectral response peak energy has a fairly small sensitivity to interdiffusion. The normal incidence excited state (E_0^1) of the interdiffused QDs remains

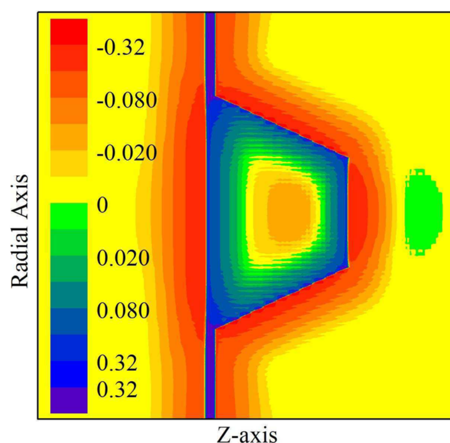

FIG. 10. The modification of the potential of QD3 due to diffusion of 10 Å. The potential profile is taken through the center of the QD. The decrease in the potential within the center of the QD is due to a relaxation of the strain.

deeply confined and is therefore unlikely to contribute to the photocurrent of QDIPs. To develop a QDIP that has an inherent normal incidence absorption, novel QD growth techniques are required which place the E_0^1 state near the barrier band edge, such as submonolayer deposition.[35]

Making a direct comparison between the calculated band structure of interdiffused QDs and reports on experimental studies of interdiffused QDIPs is difficult since the degree of intermixing of annealed QDs is often unknown. Calculating the diffusion length induced by annealing QDs is often impossible since the diffusion processes is heavily dependent on any disorder such as point defects which might be present as well as the QD strain. However, the general dependence of QDIP spectral response on annealing can be compared with the calculated results presented here. In almost all cases, annealing results in a red shifting of the measured spectral response of In(Ga)As/GaAs QDIPs which is in agreement with calculation. The annealed $In_{0.5}Ga_{0.5}As$ QDIP reported in Ref. 36 displays a spectral response peak energy shift from 202 meV (6.2 μm) to 167 meV (7.4 μm) for a 30 s anneal at 800 °C. Assuming the QDs have a similar geometry to QD2, such an energy shift would correspond to a diffusion length of between 5 and 10 Å. The QDs of the QDIP annealed in Ref. 5 have a similar geometry to QD2 with the addition of thin $In_{0.15}Ga_{0.85}As$ QWs inserted above and below the QDs which is expected to have a minor impact on the spectral response. An 850 °C anneal red shifts the spectral response peak from 177 meV (7.0 μm) to 134 meV (9.3 μm) which corresponds to a diffusion length of about 10 Å.

It should be noted that depending on the growth conditions it is expected that QDs will in general have a nonuniform indium distribution[37,38] and interdiffusion might not strictly follow a Fickian model.[39] However, the results presented here are expected to provide a good qualitative and a somewhat quantitative guide to the effects of interdiffusion on the conduction band absorption spectra of In(Ga)As QDs.

Downloaded 14 Sep 2012 to 150.203.178.114. Redistribution subject to AIP license or copyright; see http://jap.aip.org/about/rights_and_permissions

IV. CONCLUSIONS

In summary, the effects of interdiffusion on the conduction band absorption spectrum of In(Ga)As/GaAs QDs have been calculated within the single band effective mass model with the effects of QD strain taken into consideration through solution of an elastic continuum model by a finite element method. It was found that the lack of QD symmetry in the growth direction and the presence of the wetting layer can result in a broad in-plane polarized QD absorption spectrum, even for QDs that predominantly feature bound-to-bound transitions. In general, interdiffusion results in a significant reduction of the in-plane polarized absorption spectrum peak energy for all QD geometries studied. For QDs that feature bound-to-continuum in-plane polarized transitions, interdiffusion lowers the final state energy and a single quasi bound state comes to dominate the absorption spectrum. The large strain of InAs QDs has a complicated effect on the confinement potential and it was found that interdiffusion can in-fact result in the reduction in the energy of QD states due to strain relaxation. In all cases of calculation, the total integrated absorption spectrum was found to have a very weak dependence on QD geometry or interdiffusion because the Thomas-Reiche-Kuhn f-sum rule applies to the single band effective mass model for nano-structures with a constant effective mass.

ACKNOWLEDGMENTS

Thanks are due to the Australian Research Council for the financial support of this research.

[1]R. Leon, Y. Kim, C. Jagadish, M. Gal, J. Zou, and D. J. H. Cockayne, "Effects of interdiffusion on the luminescence of InGaAs/GaAs quantum dots," Appl. Phys. Lett. **69**, 1888–1890 (1996).

[2]O. B. Shchekin, D. G. Deppe, and D. Lu, "Fermi-level effect on the interdiffusion of InAs and InGaAs quantum dots," Appl. Phys. Lett., **78**, 3115–3117 (2001).

[3]S. J. Xu, X. C. Wang, S. J. Chua, C. H. Wang, W. J. Fan, J. Jiang, and X. G. Xie, "Effects of rapid thermal annealing on structure and luminescence of self-assembled InAs/GaAs quantum dots," Appl. Phys. Lett. **72**, 3335–3337 (1998).

[4]H. S. Djie, O. Gunawan, D.-N. Wang, B. S. Ooi, and J. C. M. Hwang, "Group-III vacancy induced $In_xGa_{1-x}As$ quantum dot interdiffusion," Phys. Rev. B **73**, 155324–155329 (2006).

[5]G. Jolley, L. Fu, H. H. Tan, and C. Jagadish, "Effects of annealing on the spectral response and dark current of quantum dot infrared photodetectors," J. Phys. D **41**, 215101–215107 (2008).

[6]P. Aivaliotis, E. A. Zibik, L. R. Wilson, J. W. Cockburn, M. Hopkinson, and R. J. Airey, "Tuning the photoresponse of quantum dot infrared photodetectors across the 8-12 μm atmospheric window via rapid thermal annealing," Appl. Phys. Lett. **91**, 143502 (2007).

[7]B. Aslan, C. Y. Song, and H. C. Liu, "On the spectral response of quantum dot infrared photodetectors: Postgrowth annealing and polarization behaviors," Appl. Phys. Lett. **92**, 253118–253120 (2008).

[8]S. Mokkapati, H. H. Tan, and C. Jagadish, "Multiple wavelength InGaAs quantum dot lasers using selective area epitaxy," Appl. Phys. Lett. **90**, 171104 (2007).

[9]L. Fu, Q. Li, P. Kuffner, G. Jolley, P. Gareso, H. H. Tan, and C. Jagadish, "Two-color InGaAs/GaAs quantum dot infrared photodetectors by selective area interdiffusion," Appl. Phys. Lett. **93**, 13504–13506 (2008).

[10]I. McKerracher, J. Wong-Leung, G. Jolley, L. Fu, H. H. Tan, and C. Jagadish, "Selective intermixing of InGaAs/GaAs quantum dot infrared photodetectors," IEEE J. Quantum Electron. **47**, 577–590 (2011).

[11]A. S. W. Lee and E. Herbert Li, "Effect of interdiffusion of quantum well infrared photodetector," Appl. Phys. Lett. **69**, 3581–3583 (1996).

[12]E. H. Li, "The effect of interdiffusion on the intersubband optical properties in a modulation-doped quantum-well structure," IEEE J. Quantum Electron. **34**, 1155–1161 (1998).

[13]J. Micallef, E. H. Li, and B. L. Weiss, "Effects of interdiffusion on the sub-band-edge structure of $In_{0.53}Ga_{0.47}As$/lnP single quantum wells," J. Appl. Phys. **73**, 7524–7532 (1993).

[14]R. K. Kupka and Y. Chen, "Excitonic binding energies in diffused-intermixed GaAs/AlAs/AlGaAs double barrier quantum wells," J. Appl. Phys. **77**, 1990–1998 (1995).

[15]S. Panda, B. K. Panda, S. Fung, and C. D. Beling, "Electric field effect on the diffusion modified AlGaAs/GaAs single quantum well," J. Appl. Phys. **80**, 1532–1540 (1996).

[16]P. J. Hughes, B. L. Weiss, and H. E. Jackson, "Composition and confinement energies of interdiffused AlGaAs/GaAs single quantum well structures," Semicond. Sci. Technol. **12**, 808–812 (1997).

[17]K. S. Chan, E. Herbert Li, and M. C. Y. Chan, "Optical gain of interdiffused InGaAs/GaAs and AlGaAs/GaAs quantum wells," IEEE J. Quantum Electron. **34**, 157–165 (1998).

[18]M. Srujan, K. Ghosh, S. Sengupta, and S. Chakrabarti, "Presentation and experimental validation of a model for the effect of thermal annealing on the photoluminescence of self-assembled InAs/GaAs quantum dots," J. Appl. Phys. **107**, 123107–123113 (2010).

[19]J. A. Barker and E. P. O'Reilly, "The influence of inter-diffusion on electron states in quantum dots," Physica E **4**, 231–237 (1999).

[20]O. Gunawan, H. S. Djie, and B. S. Ooi, "Electronics states of interdiffused quantum dots," Phys. Rev. B **71**, 205319 (2005).

[21]D. Biswas, S. Kumar, and T. Das, "Interdiffusion induced changes in the photoluminescence of $In_XGa_{1-X}As$/GaAs quantum dots interpreted," J. Appl. Phys. **101**, 026108–026110 (2007).

[22]N. Vukmirović, Ž. Gačević, Z. Ikonić, D. Indjin, P. Harrison, and V. Milanović, "Intraband absorption in InAs/GaAs quantum dot infrared photodetectors: Effective mass versus $k \times p$ modelling," Semicond. Sci. Technol. **21**, 1098–1104 (2006).

[23]I. Vurgaftman, J. R. Meyer, and L. R. Ram-Mohan, "Band parameters for III-V compound semiconductors and their alloys," J. Appl. Phys. **89**, 5815–5875 (2001).

[24]M. A. Cusack, P. R. Briddon, and M. Jaros, "Electronic structure of InAs/GaAs self-assembled quantum dots," Phys. Rev. B **54**, R2300–R2303 (1996).

[25]H. C. Liu, "Dependence of absorption spectrum and responsivity on the upper state position in quantum well intersubband photodetectors," J. Appl. Phys. **73**, 3062–3067 (1993).

[26]P. Bhattacharya, S. Ghosh, and A. D. Stiff-Roberts, "Quantum dot opto-electronic devices," Annu. Rev. Mater. Res. **34**, 1–40 (2004).

[27]M. S. Skolnick and D. J. Mowbray, "Self-assembled semiconductor quantum dots: Fundamental physics and device applications," Annu. Rev. Mater. Res. **34**, 181–218 (2004).

[28]S. Chakrabarti, S. Adhikary, N. Halder, Y. Aytac, and A. G. U. Perera "High-performance, long-wave (10.2 μm) InGaAs/GaAs quantum dot infrared photodetector with quaternary $In_{0.21}Al_{0.21}Ga_{0.58}As$ capping," Appl. Phys. Lett. **99**, 181102 (2011).

[29]X. Lu, J. Vaillancourt, M. J. Meisner, and A. Stintz "Long wave infrared InAs-InGaAs quantum-dot infrared photodetector with high operating temperature over 170K," J. Phys. D **40**, 5878–5882 (2007).

[30]S.-Y. Lin, J.-Y. Chi, and S.-C. Lee, "High responsivity quantum dot infrared photodetector with $Al_{0.1}Ga_{0.9}As$ blocking layers at both sides of the structure," J. Cryst. Growth **278**, 351–354 (2005).

[31]Z. Ye, J. C. Campbell, Z. Chen, E. T. Kim, and A. Madhukar, "InAs quantum dot infrared photodetectors with $In_{0.15}Ga_{0.85}As$ strain-relief cap layers," J. Appl. Phys. **92**, 7462–7468 (2002).

[32]D. Pan, E. Towe, and S. Kennerly, "A five-period normal-incidence (In, Ga)As/GaAs quantum-dot infrared photodetector," Appl. Phys. Lett. **75**, 2719–2721 (1999).

[33]J. Phillips, P. Bhattacharya, S. W. Kennerly, D. W. Beekman, and M. Dutta, "Self-assembled InAs/GaAs quantum-dot intersubband detectors," IEEE J. Quantum Electron. **35**, 936–943 (1999).

[34]L. Fu, P. Lever, K. Sears, H. H. Tan, and C. Jagadish, "$In_{0.5}Ga_{0.5}As$/GaAs quantum dot infrared photodetectors grown by metal-organic chemical vapor deposition," IEEE Electron Device Lett. **26**, 628–630 (2005).

[35]D. Z.-Y. Ting, S. V. Bandara, S. D. Gunapala, J. M. Mumolo, S. A. Keo, C. J. Hill, J. K. Liu, E. R. Blazejewski, S. B. Rafol, and Y.-C. Chang, "Submonolayer quantum dot infrared photodetector," Appl. Phys. Lett. **94**, 111107 (2009).

[36]L. Fu, H. H. Tan, I. McKerracher, J. Wong-Leung, C. Jagadish, N. Vukmirović, and P. Harrison, "Effects of rapid thermal annealing on device

Downloaded 14 Sep 2012 to 150.203.178.114. Redistribution subject to AIP license or copyright; see http://jap.aip.org/about/rights_and_permissions

characteristics of InGaAs/GaAs quantum dot infrared photodetectors," J. Appl. Phys. **99**, 114517 (2006).

[37]I. Kegel, T. H. Metzger, A. Lorke, J. Peisl, J. Stangl, G. Bauer, J. M. García, and P. M. Petroff, "Nanometer-scale resolution of strain and interdiffusion in self-assembled InAs/GaAs quantum dots," Phys. Rev. Lett. **85**, 1694–1697 (2000).

[38]N. Matsumura, T. Haga, S. Muto, Y. Nakata, and N. Yokoyama, "Lattice deformation and interdiffusion of InAs quantum dots on GaAs (100)," J. Appl. Phys. **89**, 160–164 (2001).

[39]A. Babinski and J. Jasinski, "Post-growth thermal treatment of self-assembled InAs/GaAs quantum dots," Thin Solid Films **412**, 84–88 (2002).

Downloaded 14 Sep 2012 to 150.203.178.114. Redistribution subject to AIP license or copyright; see http://jap.aip.org/about/rights_and_permissions